Chapter 6
Shelf-Break Exchange in the Bering, Chukchi and Beaufort Seas

William J. Williams, Emily Shroyer, Jaclyn Clement Kinney, Motoyo Itoh, and Wieslaw Maslowski

Abstract The Bering and Chukchi/Beaufort shelf-breaks form the beginning and end of the dramatic sea-level and wind-forced flow of Pacific Ocean water across the Bering and Chukchi continental shelves between the Pacific and Arctic Oceans. Recent model results suggest that the on-shelf flow in the Bering is distributed along the shelf-break, wind-dependant, focused by Zhemchug and Bering canyons and modified by shelf-break eddies. Similarly, the off-shelf flow in the Chukchi/Beaufort is mediated by canyons, shelf-break jets, eddies, and wind forcing. In the Chukchi, flow is channeled through Barrow and Herald canyons to the shelf-break, where across-slope flow in Ekman boundary layers and instabilities result in the exchange of water and properties across the slope. In addition, dense shelf-water, created from brine rejection during ice formation in coastal polynyas, has been observed to flow downslope through Barrow Canyon. Along the Beaufort shelf, the shelf-break current is unstable, shedding eddies that populate the deep Beaufort basin. Upwelling favorable winds in summer have been observed to modify the structure of the shelf-break current and drive exchange across the Chukchi and Beaufort slopes. Most of

W.J. Williams (✉)
Fisheries and Oceans Canada, Institute of Ocean Sciences, Sidney, BC, Canada V8L 4B2
e-mail: Bill.Williams@dfo-mpo.gc.ca

E. Shroyer
College of Oceanic and Atmospheric Sciences, Oregon State University,
104 COAS Administration Building, Corvallis, OR 97331-5503, USA
e-mail: eshroyer@coas.oregonstate.edu

J. Clement Kinney • W. Maslowski
Department of Oceanography, Graduate School of Engineering and Applied Sciences,
Naval Postgraduate School, Monterey, CA 93943, USA
e-mail: jlclemen@nps.edu; maslowsk@nps.edu

M. Itoh
Japan Agency for Marine-Earth Science and Technology, Yokosuka-city,
Kanagawa 237-0061, Japan
e-mail: motoyo@jamstec.go.jp

J.M. Grebmeier and W. Maslowski (eds.), *The Pacific Arctic Region: Ecosystem Status and Trends in a Rapidly Changing Environment*, DOI 10.1007/978-94-017-8863-2_6,

our understanding of shelf-break flow in Bering and Chukchi Seas is based on numerical model results and broad-scale observations. There is thus a need for more detailed shelf-break observational programs.

Keywords Shelf-break • Canyon • Bering Sea • Chukchi Sea • Beaufort Sea • Polynya

6.1 Introduction

The shelf-break at the edge of a continental shelf is a transition region between the shallow shelf and the much deeper slope and basin. In comparison to basins, shelves are directly influenced by river inflow and their shallowness strongly amplifies the response to tidal and wind-forcing. The rapid increase in bottom slope at the shelf-break, from the relatively flat continental shelf to the much steeper slope, forms a barrier to rotationally dominated (i.e. geostrophically balanced) flows, which are strongly constrained to flow along, rather than across isobaths and changes the interaction of stratified flow with the bathymetry. Since the shelf-break delineates all these basic differences, fronts, eddies and jets contribute to significant variability at the shelf-break. In addition, the shelf-break is incised by a wide range of undersea canyons formed during glacial periods of low sea level by river runoff and glaciation. The interaction of shelf-break flows and eddies with these canyons results enhanced shelf-break exchange of mass, heat, salt, and other tracers.

Shelf-breaks can be characterized by their depth, width and topographic variations such as undersea headlands and canyons, where the width is the transition from the bottom slope of the shelf to that of the slope. The shelf-break of the Bering, bounded by the Aleutian Islands in the southeast and Siberia in the northwest, is ~150–200 m deep and contains a number of large cross shelf canyons of which Zhemchug Canyon dominates the central shelf and Pribilof and Bering canyons influences the southeastern shelf (Fig. 6.1a). The Chukchi shelf-break, between Herald Canyon in the west and Barrow Canyon in the east, is ~75 m deep and varies from ~20 km wide in the east to being very broad in the west (Fig. 6.1b). The Alaskan Beaufort Shelf, east of the Chukchi Sea, sits between Barrow Canyon and Mackenzie Trough and its shelf-break is only 60 m deep and very sharp – the transition from shelf to slope is only ~5 km wide (Fig. 6.1c).

The Bering and Chukchi/Beaufort shelf-breaks are also unique in that they are the beginning and end of the flow of Pacific-origin water from the deep Bering Sea through Bering Strait to the Canadian Basin of the Arctic Ocean. This sea-level and wind-forced flow across the broad continental shelves of the Bering and Chukchi forms an advective highway on which there is high biological production fed from the nutrients within the Pacific-origin water. To balance the northward flow through Bering Strait, there is on-shelf flow across the Bering shelf-break in addition to the along-shelf flow through the Unimak Pass in the Aleutian Island Chain. The Bering Strait through-flow crosses the Chukchi Sea, becoming off-shelf flow across the Chukchi-Beaufort shelf-break, as the Pacific water spills off the shelf and into the surface layers and halocline of the Canadian Basin. The on-shelf flow in the Bering

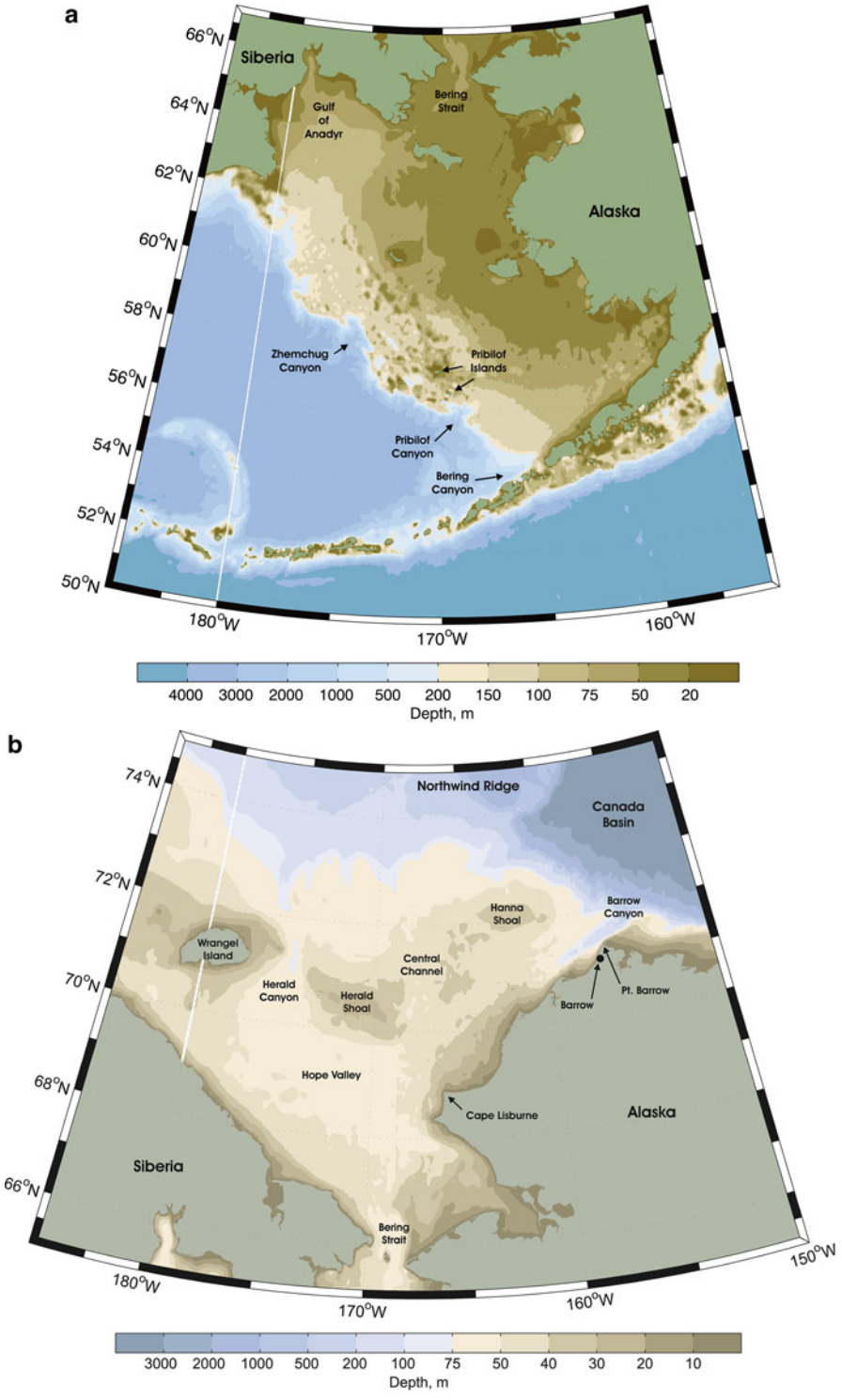

Fig. 6.1 Maps of (**a**) the Bering Sea (**b**) the Chukchi Sea and (**c**) the Alaskan Beaufort Shelf. The bathymetry changes color to highlight the shelf-break and canyons. In (**c**) the *black dots* at the mouth of Barrow Canyon show the location of the mooring data used in Figs. 6.12 and 6.13

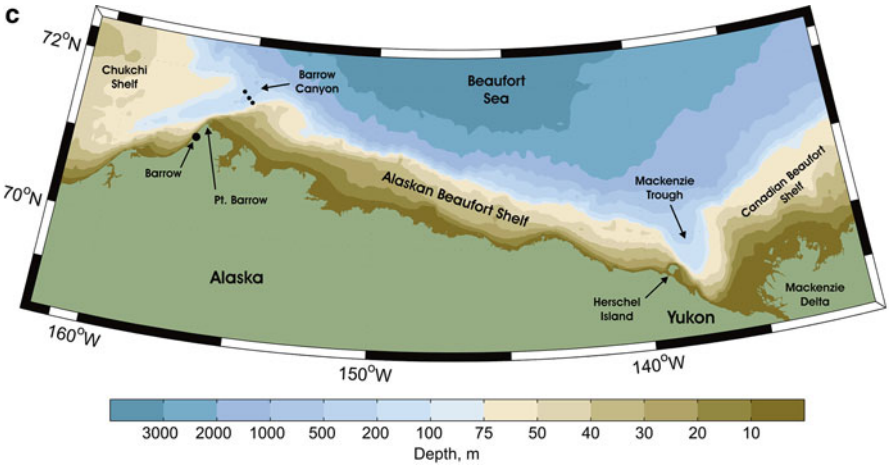

Fig. 6.1 (continued)

Sea has typically been thought of as occurring in the northwest near the Gulf of Anadyr, but see Fig. 6.2 below for modeling results.

This chapter reviews our historical and current understanding of on- and off-shelf flows at the Bering and Chukchi/Beaufort shelf-breaks, including contributions from eddies and wind-driven upwelling and downwelling, and, for the Chukchi/Beaufort the production of dense shelf water in coastal polynyas and its subsequent flow across the shelf-break. Particular attention is paid to the role that the many canyons play in enhancing shelf-break exchange in this region. In general, shelf-break exchange can be driven by an even larger range of processes, including the above as well as tidal dynamics (both barotropic and baroclinic), frontal meanders, filaments, and intrusions, bottom boundary layer friction, and coastally trapped waves (Huthnance 1995). For the generation of eddies by instabilities, the interaction of eddies with the shelf-break and canyons, and the interaction of along-shelf flow with canyons the constraint that geostrophic flow follows isobaths is broken by the non-linear terms in the momentum equation further modified by stratification. In addition spatial variability in wind stress and Ekman transport (for example that introduced by the coastline) leads to convergence/divergence on the shelf and consequent onshelf/offshelf flow.

6.2 The Bering Shelf-Break

The earliest suggestions of exchange between the basin and shelf in the Bering Sea can be inferred from charts of generalized surface circulation schemes proposed by a number of researchers in the mid-twentieth century (see Hughes et al. 1974 for a review). Because these early circulation charts were typically derived from

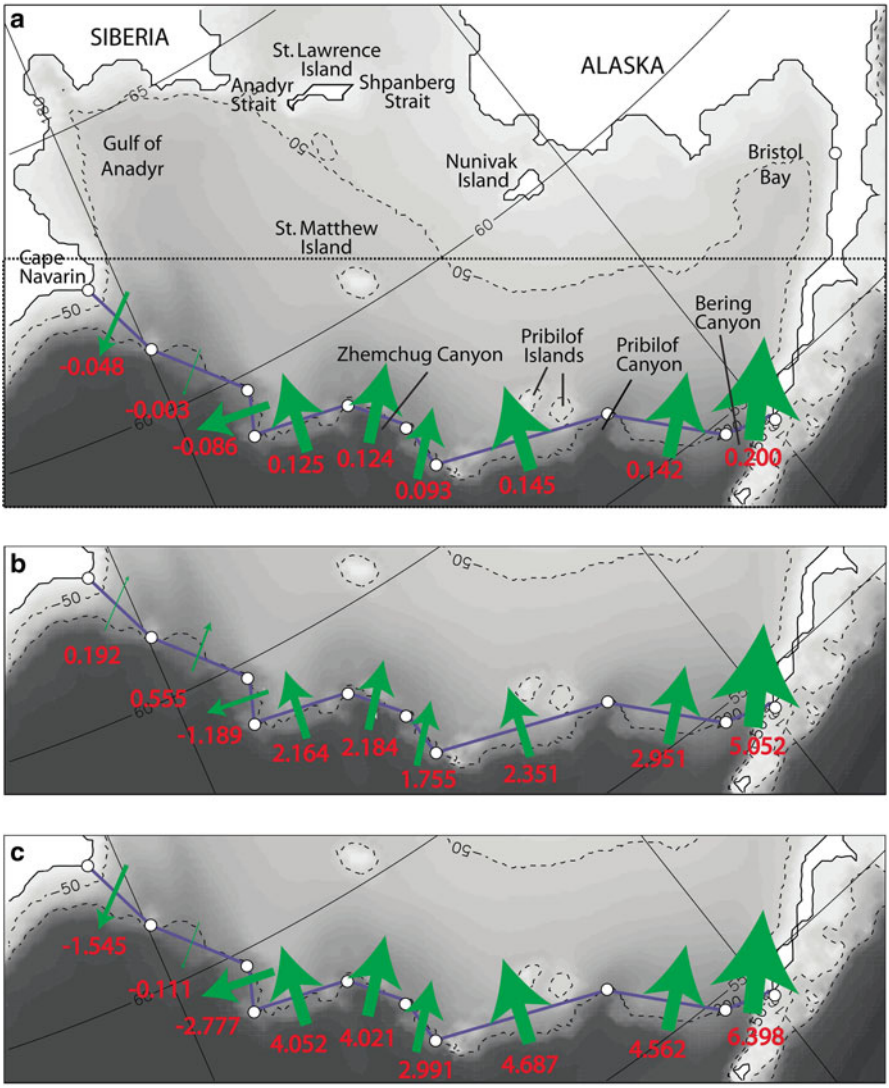

Fig. 6.2 Twenty six year (1979–2004) mean (**a**) volume transport (Sv), (**b**) heat flux (TW; relative to −1.9 °C) and (**c**) salt flux (10^6 kg/s) across various sections along the Bering shelf-break using output from the NAME numerical model. *Arrows* indicate net direction (positive is North or West) and are scaled relative to the largest value in each Figure. The *shading* indicates depth (m). The 50 m and 200 m isobaths are shown as *dotted lines* (Figure adapted from Fig. 3 of Clement Kinney et al. (2009) with permission from Elsevier)

compilations of disparate, temporally- and spatially-limited data sets, the depicted exchange pathways between basin and shelf were rudimentary at best.

A significant improvement to our understanding of basin-shelf exchange in the Bering Sea occurred with the description of the Bering Slope Current (BSC)

system (Kinder et al. 1975). A transport budget derived from continuity constraints on geostrophic transport calculations for the BSC implied the existence of large exchanges between basin and shelf, exceeding 1 Sv, that were proposed to preferentially occur in association with the large submarine canyons incising the continental slope. Additionally, the authors proposed that the BSC could be characterized as a system of mesoscale eddies that exhibits seasonal modulation. Both these aspects of the BSC, the eddies and the canyons, have been found to be important to shelf-basin exchange.

Kinder and Coachman (1978) estimated cross-shelf exchange through consideration of the persistent haline front that overlies the 1,000-km long continental slope in the central Bering Sea. Maintenance of this front was found to require a ~5×10^4 kg s^{-1} shoreward, tidally-driven diffusion of salt. Using the best estimates of Bering Strait transport, mean salinity, and freshwater runoff available at the time, they also computed a salt and freshwater balance for the entire Bering Shelf from which an on-shelf advective salt flux of 4.9×10^7 kg s^{-1} was estimated. This is approximately 1,000 times the estimated flux required to maintain the shelf-break haline front within the central Bering. They inferred that most of this advective salt flux occurs near the Siberian coast, where the haline front is poorly defined, and then passes directly through the Gulf of Anadyr to Bering Strait. This supported a previous paper by Coachman et al. (1975), which was the first to show hydrography that clearly indicated flow around the Gulf of Anadyr, implying shelf-basin exchange near the Siberian coast.

Although not explicitly identified as such, a broad-scale indicator of on-shelf (heat) transport in the Bering Sea was inferred from Pease (1980). She first identified that southwestward ice advection driven by northerly winds coupled with ice melt at the thermodynamic limit of the southern ice-edge are the principal processes that influence sea ice production and extent in the Bering Sea. She further suggested that inter-annual changes in sea ice extent were dependent upon the interplay of these processes and thus dependent on the heat flux to the Bering shelf from the deep basin.

Although Kinder et al. (1980) reported on a satellite-tracked drifter that circumscribed an eddy and then moved onto the shelf, Paluszkiewicz and Niebauer (1984), using satellite imagery of sea surface temperature, and Karl and Carlson (1987), using distributions of suspended sediments, were the first to implicate both (1) mesoscale eddies as agents promoting exchange between basin and shelf in the Bering Sea and (2) submarine canyons as locations of enhanced eddy-induced basin-shelf exchange. Paluszkiewicz and Niebauer (1984) provide rough estimates for the temporal (2–6 months) and spatial (order 100 km) scales of the BSC eddy field using satellite imagery and suggest the variability in the eddy field was associated with changes in flow through the passes between the eastern Aleutian Islands. Okkonen (2001) later used 4 years of TOPEX satellite altimeter data to refine these estimates and show that the most energetic activity in the BSC eddy field typically occurs in the spring and summer months and is characterized by along-slope wavelengths of ~200 km and wave periods of ~4 months.

The first direct evidence for shelf-slope exchange in the Bering Sea was acquired by moored instruments deployed at slope and mid-slope locations in Pribilof Canyon, Zhemchug Canyon, and midway between these canyon sites (Schumacher and Reed 1992). Whereas computed momentum and heat fluxes indicated both on-shelf and off-shelf flows, salt fluxes were preferentially on-shelf. Schumacher and Stabeno (1994) re-examined these data in conjunction with satellite-tracked drifter trajectories from the southeast Bering Sea and concluded that the current reversals and coincident shelf-slope exchanges of water properties were due to the passage of small (<25 km) eddies at periodicities of 45–60 days. Subsequent satellite-tracked drifter studies also indicated an association between eddies and on-shelf flow (Stabeno and van Meurs 1999; Stabeno et al. 1999).

Mizobata and Saitoh (2004) used 3 years (1998–2000) of satellite measurements of sea surface height anomalies, ocean color and sea surface temperature to show that surface chlorophyll concentrations and primary production along the outer shelf and above the continental slope in the central Bering Sea were enhanced when the variability of the BSC eddy field was elevated. They attributed elevated eddy field variability to increased transport in the BSC fed by increased transports of the Alaskan Stream and Aleutian North Slope Current. Okkonen et al. (2004) used satellite images of ocean color to illustrate eddy-induced on-shelf intrusions of low chlorophyll basin water and off-shelf entrainment of high chlorophyll shelf water.

These observational findings were complemented by the modeling efforts of Mizobata et al. (2006), who used a 5-km resolution numerical model of the southeastern Bering Sea to study eddy-induced exchange between basin and shelf. Results showed that subsurface, on-shelf nutrient flux was greater when eddies were adjacent to the shelf-break than when absent from the shelf-break region. Model results also showed that surface waters from the outer shelf were transported ~100 km into the basin by shelf-break eddies.

Models have also been used to constrain the total mean volume and property transport budgets across the outer Bering Sea shelf (defined between the 50-m and 200-m isobaths), Clement et al. (2009) analyzed output from the Naval Postgraduate School Arctic Modeling Effort ice-ocean model (NAME; see e.g. Maslowski et al. 2004, 2014, this volume). This model has ~9 km horizontal resolution and 45 levels in the vertical. The horizontal resolution permits eddies as small as 36 km. The model was first spun-up for 21 years using ECMWF winds and then the final run used realistic daily-averaged ECMWF forcing beginning in 1979 and continuing through 2004. A series of cross-shelf sections along the shelf break of the long-term (1979–2004) mean volume, heat, and salt transports from NAME are shown in Fig. 6.2. Figure 6.2a shows the 26-year mean value of volume transport, in Sv (1 Sv = 10^6 m^3/s), across each section with an arrow indicating the mean direction of flow. Arrows are scaled as a percentage of the largest cross-sectional value shown in the figure (e.g. a volume transport of 0.2 Sv would have an arrow twice as wide as a section with a volume transport of 0.1 Sv). Along the central and eastern part of the slope, we can see that the net volume transport is positive (on-shelf); however the western part of the slope shows relatively small negative (off-shelf) values.

Table 6.1 Twenty-six-year (1979–2004) mean on-shelf, off-shelf, and net volume, heat and salt transport across the sections shown in Fig. 6.2, which approximate the 200 m isobath

Parameter	On-shelf	Off-shelf	Net
Volume transport (Sv)	0.829	−0.137	0.692
Heat transport (TW)	17.204	−1.189	16.015
Salt transport (10^6 kg/s)	26.711	−4.433	22.278

The Bering Slope Current tends to separate from the shelf-break west of Zhemchug Canyon, thereby allowing off-shelf transports for sections further west (Clement Kinney et al. 2009). The mean total on-shelf, off-shelf and net volume transports are 0.829 Sv (S.D. = 0.728 Sv), −0.137 Sv (S.D. = 0.384 Sv), and 0.692 Sv (S.D. = 0.421 Sv), respectively (Table 6.1). The net on-shelf volume transport is the mean flow though Bering Strait in the model, and comparable to the observed Bering Strait through-flow of ~0.8 Sv (Woodgate et al. 2006). However, Aagaard et al. (2006), in a volume and salinity balance for the Bering Shelf, found on-shelf volume transport to be roughly equally split between the flow of the Alaskan Coastal Current through Unimak Pass (the first opening in the Aleutian Island chain) and on-shelf flow across the shelf-break, highlighting the need for observations of shelf-break exchange in the Bering and of the flow through Unimak Pass and subsequent gaps in the Aleutian Island chain. Note that these modeling results are in contrast to the historical notions of the Bering Strait through-flow crossing the Bering shelf-break in the Gulf of Anadyr (e.g. Coachman et al. 1975) which warrants further investigation, such as Danielson et al. (2012).

The long-term mean heat transports, calculated using a reference temperature of −1.9 °C, are shown in Fig. 6.2b. The largest on-shelf oceanic heat flux is through Zhemchug Canyon (a total of 6.1 TW through the three sections that encompass Zhemchug Canyon), with the second largest on-shelf heat flux through Bering Canyon (5.1 TW). The mean total on-shelf, off-shelf and net heat transports are 82.2432 TW (S.D. = 30.718 TW), 56.542 TW (S.D. = 19.894 TW) and 25.701 TW (S.D. = 17.447 TW), respectively. The mean salt transports through the sections along the 200-m isobath (Fig. 6.2c) follow the mean volume transports, due to the strong dependence of salt transport on volume transport. The mean total on-shelf, off-shelf, and net volume, heat and salt transports are given in Table 6.1.

Danielson et al. (2012) break down the long-term mean view by considering the response of the Bering Shelf to no-wind or along-shelf wind that is either northwesterly (upwelling favorable) or southeasterly (downwelling favorable). They illustrate the effect of wind-direction using a one layer idealized barotropic model and linearized bottom friction (Fig. 2 in Danielson et al. 2012). Under no-wind conditions, the model shows the Bering Strait source waters to cross the shelf-break in the Gulf of Anadyr, similar to a study by Kinder et al. (1986) that suggested the notion of topographic beta effect focusing the flow through the Gulf of Anadyr. However, during southeasterly winds, the through-flow is spread out over the entire shelf-break, reminiscent of the long-term mean presented by Clement et al. (2009). Northwesterly wind generated off-shelf flow over most of the shelf-break that was compensated by additional on-shelf flow, with the Bering Strait through-flow, at the northwestern

end of the shelf. These results from their idealized barotropic model were also confirmed with realistic three-dimensional modeling.

Although this idealized model is instructive, the Bering shelf-break is much more complex with variation on a variety of time and space scales, e.g. those related to eddies and cross-shelf exchange in canyons. To illustrate the potential effects of the interaction of eddies and canyons on shelf-basin exchange in the Bering Sea, Figs. 6.3 and 6.4 show three cases from the NAME model (July 1987, November 1993, and May 2002) when heat and salt flux anomalies across the Zhemchug Canyon were at local maxima (see Fig. 7 of Clement Kinney et al. 2009 for time series of heat and salt flux anomalies) caused by modeled cyclonic eddies located just south of the canyon. Figure 6.3 shows that the sea surface height anomalies decrease to −20 cm (or less) in the center of these modeled cyclones. When the cyclones are present, salinities increase both near the bottom and near the surface by up to 0.4 psu and on-shelf flow occurs with speeds between 8 cm/s (July 1987) and over 14 cm/s (May 2002).

Clement Kinney et al. (2009) calculated the on shelf nutrient fluxes associated with a cyclonic eddy located over the slope at Zhemchug Canyon beginning in November 1993 (Fig. 6.3b). First the vertically integrated on-shelf salt flux, via both upwelling of relatively salty water and on-shelf flow, was calculated and then this was converted to a flux of silica using a relation between salinity and silica concentration from data in Cooper et al. (1997). It was estimated that a total of 8,350 kg of silica could be advected onto the Bering Sea shelf through Zhemchug Canyon over 3 months The transport associated with the upwelled water only (deeper than 100 m) was 2,426 kg of silica so that 70 % of the transport was in the upper water column.

Stabeno et al. (1999) suggest that high productivity in the waters surrounding the Pribilof Islands results as a consequence of flow on the outer shelf passing through the narrow space between the northern flank of Pribilof Canyon and the Pribilof Islands. Here, the flow on the outer shelf accelerates and entrains nutrient-rich slope water from Pribilof Canyon. This increase in the flow can also be seen in model results from Clement Kinney et al. (2009; see Fig. 6.2), as elevated total kinetic energy in the area between the northern flank of Pribilof Canyon and the Pribilof Islands.

It can be concluded that upwelling of nutrient-rich, deep Bering Sea water due to eddies and shelf-basin exchange enhances biological production in this region.

6.3 The Chukchi and Beaufort Shelf-Break

6.3.1 Shelf-Basin Connections

Pacific Water is a source of heat, freshwater, nutrients, and carbon for the Arctic Ocean. After passing through Bering Strait, Pacific Water must transit across the shallow, broad Chukchi before reaching the shelf-break and the edge of the deep Arctic Ocean basin. Physical mechanisms regulating shelf-break exchange control

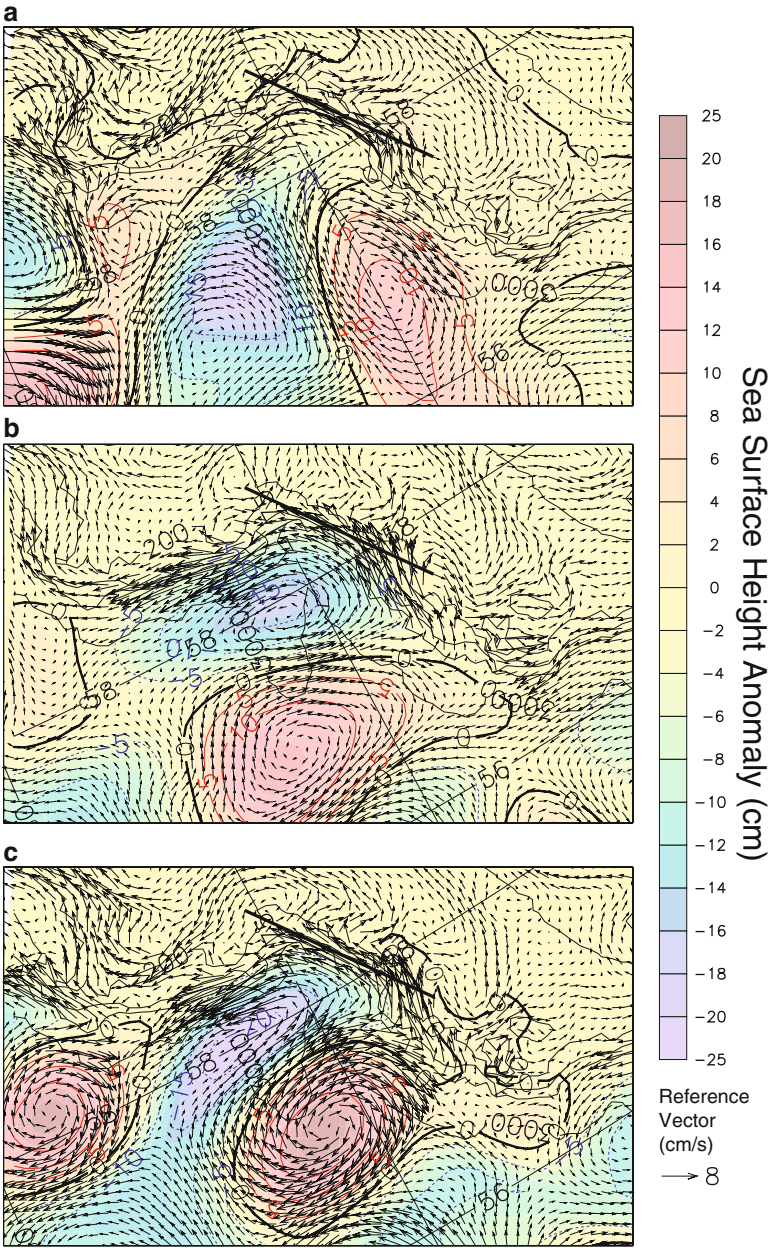

Fig. 6.3 Sea surface height anomaly (cm; *shading*) and velocity vectors (cm/s; *arrows*) averaged over the entire water column during (**a**) July 1987, (**b**) November 1993, and (**c**) May 2002 using output from the NAME numerical model. *Red* and *blue contour lines* indicate sea surface height anomalies. The location is the Bering shelf-break encompassing Zhemchug Canyon (see Fig. 6.1a). The cross-section across Zhemchug Canyon that is displayed in Fig. 6.4 is shown as a solid *black line* (Figure adapted from Fig. 8 of Clement Kinney et al. (2009) with permission from Elsevier)

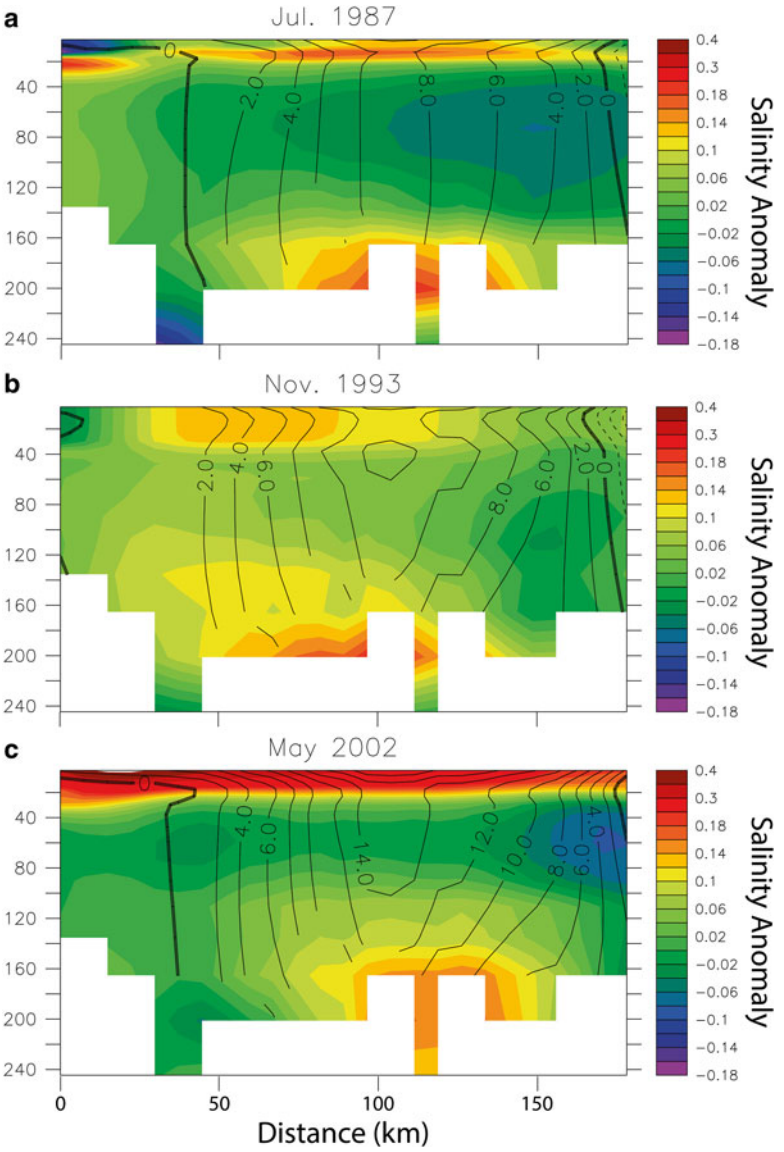

Fig. 6.4 Vertical section of salinity anomaly (*shading*) and velocity (*contours*) across Zhemchug Canyon during (**a**) July 1987, (**b**) November 1993, and (**c**) May 2002 using output from the NAME numerical model. The location of the cross-section is shown in Fig. 6.3 (Figure adapted from Fig. 9 of Clement Kinney et al. (2009) with permission from Elsevier)

how, when, and where Pacific Water enters the deep Arctic basin (see Fig. 5.3 in Chap. 5 of this volume for the mean ocean circulation pattern). Although many questions exist regarding the processes, we know that exchange between the shelf and basin occurs since Pacific Water dominates the halocline of the Canadian Basin. In the Beaufort Gyre region, for instance, Pacific Summer Water makes up a warm

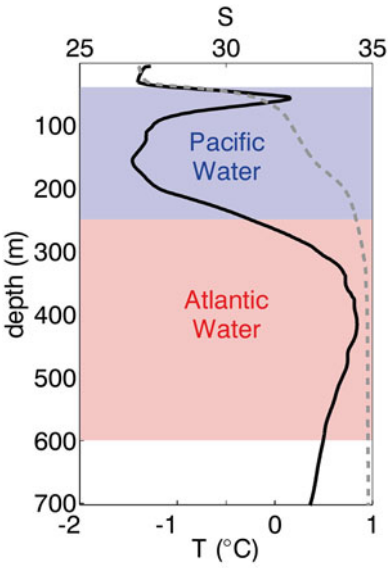

Fig. 6.5 Temperature (*solid black*) and salinity (*dashed grey*) from an ice-tethered profiler within the Canada Basin. Data show month-long average beginning May 15, 2007. The signature of warm, summer Pacific water is evident in the upper halocline. Cool, winter Pacific water contributes to water found deeper within the halocline. The Ice-Tethered Profiler data were collected and made available by the Ice-Tethered Profiler Program (Toole et al. 2011; Krishfield et al. 2008) based at the Woods Hole Oceanographic Institution (http://www.whoi.edu/itp)

layer that is regularly observed at roughly 50 m depth (e.g. Toole et al. 2010), while colder and saltier Pacific Winter Water contributes to deeper halocline layers (e.g. Aagaard et al. 1981). An example profile of temperature and salinity data acquired by an ice-tethered profiler within the Canada Basin is shown in Fig. 6.5.

Due to connections between the shelf and deep basin, variability in the circulation and conditions over the shelf and shelf-break may affect the entire Arctic. For example, Woodgate et al. (2010) suggest that the 2007 record minima in sea-ice extent may have been related to an unusually large flux of heat through the Bering Strait. The consequent lateral and basal melting of sea ice over the Chukchi shelf may have amplified the effect of local solar heating by initiating an ice-albedo feedback. Satellite imagery of ice melt and sea-surface temperature have provided striking visual records of the pathways of warm Pacific Water through the Chukchi Sea (e.g. Martin and Drucker 1997; Woodgate et al. 2010) and out into the deep Beaufort (Shimada et al. 2006; Pickart and Stossmeister 2008).

Pacific water inflow is steered by topography through the Chukchi Sea (Winsor and Chapman 2004; Weingartner et al. 2005; Woodgate et al. 2005a; Maslowski et al. 2014, this volume); and, upon reaching the shelf-break, it is generally thought that flow turns east establishing a shelf-break current along the upper Chukchi and Beaufort slopes (e.g. Mathis et al. 2007; Spall 2007; Nikolopoulos et al. 2009;

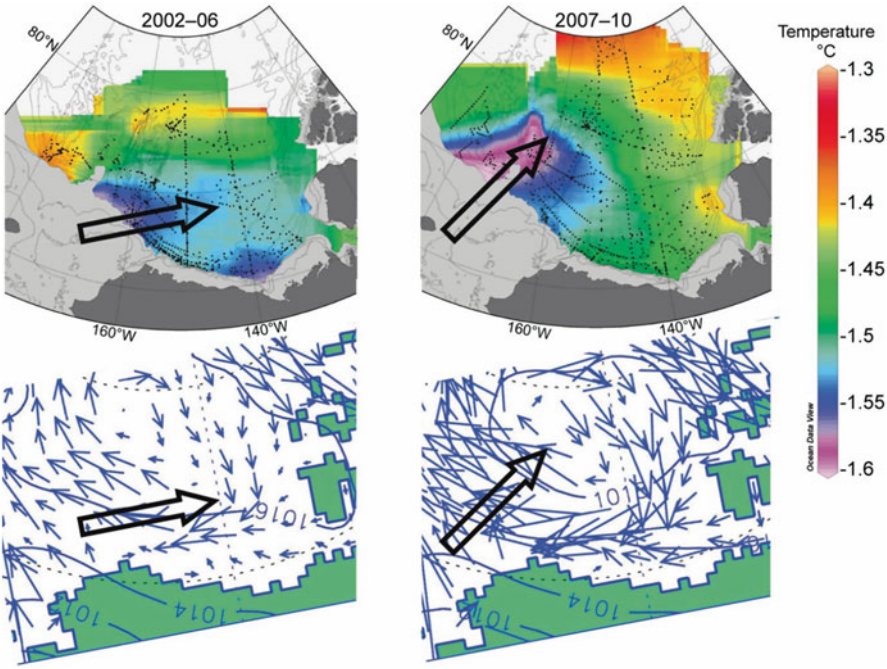

Fig. 6.6 Changes in the temperature minimum of the Pacific Winter Water in the Canadian Basin between 2002–2006 and 2007–2010 and their relationship to changes in ice motion. The *top panels* show potential temperature on the 33.1 psu isohaline to identify the core of the Pacific Winter Water and the *large arrows* suggest the direction of movement of shelf water from the Chukchi shelf-break. The *bottom panels* show sea level atmospheric pressure (hPa) and simulated wind-driven component of ice drift (Figure 5.9 from Proshutinsky et al. 2011, reproduced with permission of the American Meteorological Society)

Pickart et al. 2010). The Pacific water that is integrated into the Chukchi/Beaufort shelf-break current system enters the deep basin via eddies, filaments, or wind-driven exchange. Data from 2002 to 2004 show the annual mean volume transport within the shelf-break current at 152°W over the Alaskan Beaufort Shelf represents only 20 % of the mean transport through the Bering Strait (Nikolopoulos et al. 2009), suggesting that much of the Pacific Water enters the deep basin by crossing the Chukchi shelf-break, before it reaches the Alaskan Beaufort Shelf. Analysis of broad-scale hydrographic data from 2002 to 2010 shows the core of the Pacific Winter Water (33.1 psu) is coldest adjacent to the shelf-break of the Chukchi Sea, suggesting the greatest shelf-break exchange is in this region and thus supporting the results from 152°W. Splitting the hydrographic data into two time periods (2002–2006 and 2007–2010) shows a westward shift in the location of shelf-break exchange and the path of Pacific Winter Water in the Canadian Basin that correlates with an increase in westward mean wind and ice surface-stress (Fig. 6.6, Proshutinsky et al. 2011). The Barrow Canyon event shown in Fig. 6.9,

and further discussed below, offers an example of off shelf flow in the Chukchi, yet, the dynamics that regulate this type of breakout event are not well understood. We choose to focus this summary on those mechanisms, dynamic instabilities of the shelf-break current and wind-driven exchange, which have received more attention to-date.

6.3.2 Instabilities of the Shelf-Break Jet

The shelf-break current as measured at 152°W on the Alaskan Beaufort Shelf is relatively narrow (10–15 km) and, in the annual mean, is a bottom-intensified jet with speeds of roughly 15 cm/s (Nikolopoulos et al. 2009). The structure of the shelf-break current in this location varies greatly depending on both season and wind conditions (Nikolopoulos et al. 2009; von Appen and Pickart 2011). In winter and spring, a bottom-intensified jet carries cold Pacific Winter Water. In late summer and early fall, the shelf-break current transports warm, Pacific Summer Water often in the form of a surface-intensified jet. Strong easterlies can cause the current to completely reverse, and, although reversals may happen at anytime of year, they appear to be most common in early fall when the ocean is ice-free and easterly winds are strong (Pickart et al. 2009).

In the absence of wind, von Appen and Pickart (2011) further classify the summer configuration at 152°W into two distinct cases – a surface intensified jet carrying Alaskan Coastal Water and a bottom-intensified jet carrying weakly stratified Chukchi Summer Water. In the mean, the Alaskan Coastal Water configuration exceeded speeds of 30 cm/s near the surface. This configuration carried stratified water with maximum (mean) temperatures greater than 5 °C and salinity less than 31 psu. In contrast, the Chukchi Summer Water configuration consisted of a subsurface jet (mean velocities near 25 cm/s) with temperatures near 0 °C and salinities around 31.5 psu. These authors also summarized the mean winter condition in the absence of wind forcing (Fig. 6.7), although also a sub-surface jet, the winter-configurations transports cooler (roughly −1.5 °C) and saltier (33 psu) water in comparison to the Chukchi Summer Water configuration.

Subsurface eddies containing shelf-origin water populate the Canada Basin (e.g. Manley and Hunkins 1985; Muench et al. 2000; Timmermans et al. 2008). The majority of eddies are anticyclonic and subsurface with cold Pacific Winter Water found in their core (Krishfield et al. 2002); however, observations have also documented surface-intensified warm anticyclones composed of Alaskan Coastal Water (Pickart and Stossmeister 2008). While previous studies have suggested that Barrow Canyon may provide a localized source of eddy generation (e.g. D'Asaro 1988; Watanabe and Hasumi 2009), other studies have also shown that the shelf-break current is generally unstable without the influence of complex topography (Spall et al. 2008; von Appen and Pickart 2011).

Modeling work by Spall et al. (2008) indicates that the winter-time shelf-break jet is susceptible to baroclinic instabilities. Consistent with the numerous observations

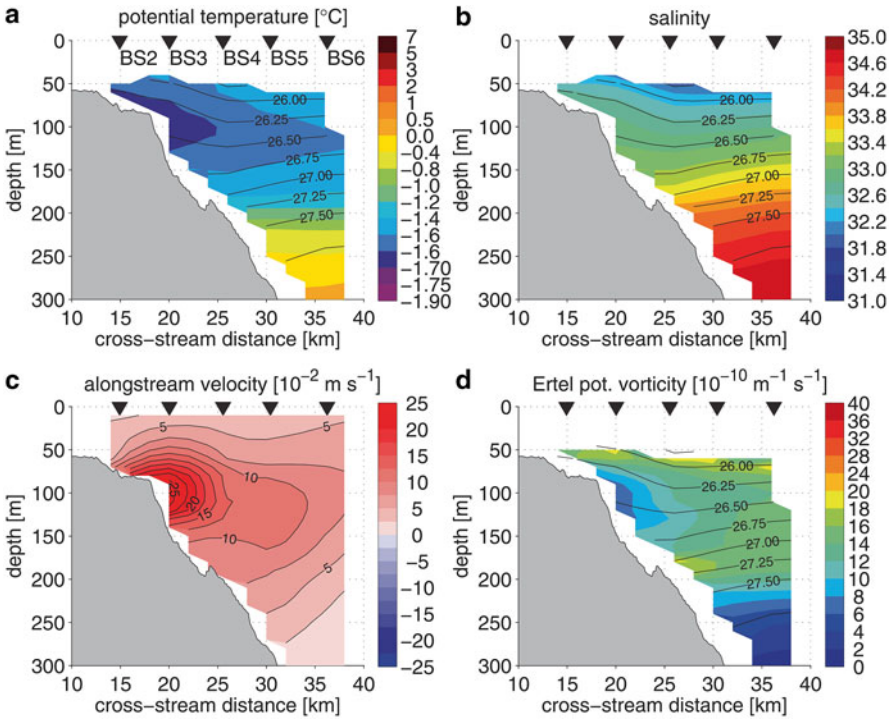

Fig. 6.7 (**a**) Temperature, (**b**) salinity, (**c**) along-shelf velocity, and (**d**) across-shelf velocity for the Pacific Winter Water configuration of the Beaufort shelf-break current (Reproduction of Fig. 10 from von Appen and Pickart 2011, with permission of the American Meteorological Society)

of eddies containing Pacific Winter Water, the modeled system sheds eddies readily. Interestingly, idealized inclusion of the Beaufort Gyre circulation further enhanced eddy production in the model, raising the possibility that the integrated wind response and circulation within the gyre feeds back into shelf-break current dynamics. Observations have also suggested that the summer-time configurations are baroclinically (both the Alaskan Coastal Water and Chukchi Summer Water configuration) and barotropically (only the Alaskan Coastal Water configuration) unstable (von Appen and Pickart 2011). Using energetics, von Appen and Pickart argue that the summer-time configurations decay over an e-folding scale of a few hundred kilometers along shelf, so that Pacific Water integrated into the shelf-break current is routed into the deep basin at some point along the Beaufort Slope. In contrast, the winter-time configuration decays slowly over a scale of ~1,400 km, raising the possibility that some Pacific Water may exit the Arctic Ocean directly via the Canadian Arctic Archipelago rather than being routed into the deep Arctic. Eddy generation throughout the year by these instabilities is likely responsible for a significant part of the mass-flux of Pacific Water from the shelf to the Canada Basin.

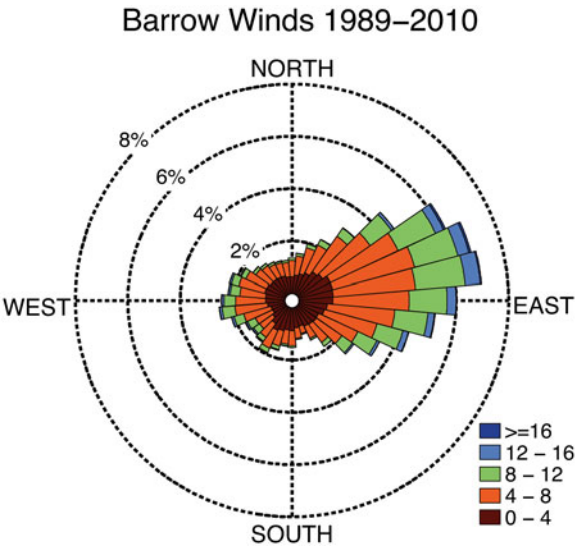

Fig. 6.8 Polar histogram showing hourly wind direction and speed from 1989 to 2010. Histogram bars point in the direction the winds originate. Data are measured 10 m above the surface at the NOAA/ESRL/GMD Pt. Barrow Observatory (http://www.cmdl.noaa.gov/info/ftpdata.html)

6.3.3 Wind-Driven Exchange

As with many places in the coastal ocean, wind-driven surface-stress is thought to play an important role in the total across-slope transport along the Chukchi and Beaufort Seas. Wind speed and direction from 1989 to 2010 at Point Barrow, Alaska are summarized in Fig. 6.8. Winds typically consist of an easterly component, which over the Chukchi/Beaufort shelf corresponds to upwelling favorable conditions. Upwelling circulation drives surface waters offshore and brings up cold, typically nutrient-rich water from depth. Upwelling of deep Atlantic Water has been regularly observed across the Chukchi and Beaufort shelves (e.g. Aagaard et al. 1981; Pickart 2004; Nikolopoulos et al. 2009); and, enhanced exchange has been indicated in canyons that cut across the slope (e.g. Carmack and Kulikov 1998; Williams et al. 2006; Mountain et al. 1976; Munchow and Carmack 1997; Weingartner et al. 1998).

Aleutian Low storm systems centered over the eastern end of the Alaskan Peninsula and Aleutian Island chain appear to be responsible for the strongest upwelling on the Beaufort Shelf (Pickart et al. 2009). Although these storms typically occur throughout the fall-winter, upwelling tends to be strongest before the onset of heavy pack ice (Pickart et al. 2009). Through the course of the year, the Chukchi and Beaufort shelves display among the largest and most variable Ekman transports within the Arctic (Yang 2006). Consistent with in situ studies, maximum upwelling occurs in November. Considering the seasonality of the winds and shelf-break current system, wind-driven exchange of Pacific Water properties (e.g. freshwater and heat) will also vary. For example, forcing of the shelf-break current in the Alaskan Coastal Water configuration by upwelling winds may contribute to significant heat transport but negligible nutrient transport. A similar wind event applied to the Winter Water configuration would result in different fluxes of heat, nutrients, and freshwater.

Pickart et al. (2011, 2013a) examined the response of the coastal current to a strong northeasterly wind event measured in November 2002. Surface-stress was enhanced during this storm due to loose ice (50–70 % concentration) responding to the wind and generating ice-ocean surface-stress higher than wind-ocean surface-stress (Pickart et al. 2013a) The westward surface-stresses were sufficient to reverse the Beaufort shelf-break jet, generating a surface intensified westward jet, and upwell Atlantic Water onto the shelf. The barotropic alongshore pressure gradient eventually 'spins-down' the reversed jet to leave behind a baroclinic structure in which upwelled Atlantic Water is integrated into a deep, eastward flowing jet that persists after the relaxation of the wind. A regional model used to interpret these observations suggests that spatial variability in ice cover, and consequently wind-stress, caused the creation of an anticyclonic gyre in the northern Chukchi. The end result being that, although upwelling and westward flow was prevalent across the Beaufort shelf and within Barrow Canyon during the storm, flow remained eastward along the Chukchi shelf. These results highlight the large temporal and spatial variability anticipated for wind forcing in this region.

Further examination of Ekman fluxes during the November 2002 storm by Pickart et al. (2013a) shows that the offshore fluxes of heat and freshwater, and onshore fluxes of nitrate are significant. For example, only 4–5 such storms can provide the nitrate needed for the estimated annual primary production of the Alaskan Beaufort Shelf. Pickart et al. (2013b) continues the analysis to show that there are 9–10 upwelling events per year that have winds greater than 10 m/s and lasting longer than 4 days. The upward nitrate flux associated with these storms during the open water season can drive primary production, and the magnitude of this storm-driven primary production is similar to that during less windy times.

6.4 Undersea Canyons of the Chukchi and Beaufort Shelves

Undersea canyons, which cut across the continental shelf, have long been noted as regions that impact not only coastal circulation but also biological productivity and sediment transport. The complex topography of canyons introduces along-shelf variation to the physical system which leads to enhanced across-shelf exchange. The circulation within and around canyons is influenced by a variety of processes, including internal wave activity and mixing, modification of coastally-trapped waves, and topographic steering of coastal currents. In turn, these physical processes influence the ecosystem by controlling sediment transport and suspension, and creating an environment that is often favorable for biological productivity. Not surprisingly, previous studies from the Chukchi and Beaufort suggest that canyons have a profound effect on the circulation and ecosystem in the Pacific Arctic.

Here, we examine the circulation in and around three canyons, two of which are found on the Chukchi Shelf, Herald and Barrow Canyon, and one of which cuts across the Canadian Beaufort Shelf, Mackenzie Trough. All three of these canyons cut across the shelf-break isobaths, yet all three differ from one another in essential

ways. A primary difference between the Chukchi canyons as compared to Mackenzie Trough is due to the physical set-up, in particular the incident angle of the primary flow. Herald and Barrow Canyons extend off the wide, shallow Chukchi Sea; and, because of northward inflow at the Bering Strait, significant along-canyon flow is anticipated and observed in these two cases even in the absence of wind. For Herald Canyon, the primary topography is on the shelf and above the isobath of the shelf-break. Thus Herald Canyon is considered to channel part of the Bering Strait through-flow and deliver it to the shelf-break and so modify the distribution of Pacific Origin water at the edge of the Chukchi Shelf. For Barrow Canyon, most of the topography is below the shelf break and the constriction in the isobaths (steep topography) against Point Barrow leads to down-canyon flow. In contrast to both of the Chukchi canyons, the axis of Mackenzie Trough runs perpendicular to the Beaufort shelfbreak current. Along-canyon transport in Mackenzie Trough, and shelf-break exchange, is found to be strongly influenced by wind-driven along-shelf flow and along-shelf dynamics (e.g. meanders in the Beaufort Slope Current or eddies).

6.4.1 Herald Canyon

Herald Canyon is located on the western Chukchi shelf along the eastern side of Wrangel Island. Its axis is primarily aligned north-south and the mouth of Herald Canyon opens at roughly the 150-m isobath on the slope separating the Chukchi Sea from the Chukchi Abyssal Plain. In comparison to the eastern Chukchi, observational work has been limited in Herald Canyon; however, the general character of the current structure and water mass properties in the canyon has been documented by a handful of studies.

Herald Canyon creates a conduit for Pacific Water from the Bering Strait toward the shelf-break of the Chukchi (Winsor and Chapman 2004; Woodgate et al. 2005a; Spall 2007) rather than directly influencing shelf-break exchange. The Pacific Water tends to occupy the eastern flank of the canyon (e.g. Woodgate et al. 2005a) and, upon exiting the canyon, is thought to turn eastward following the shelf-break (e.g. Mathis 2007; Spall 2007; Maslowski et al. 2014, this volume). In winter, the canyon is occupied by Bering Winter Water that has cooled slightly en-route through the Chukchi (Woodgate et al. 2005a). In summer, relatively warm Pacific-origin water and remnant winter water, which is believed to be formed via cooling and brine rejection within the Chukchi Sea (Kirillova et al. 2001; Weingartner et al. 2005), co-exist in Herald Canyon. These water masses are divided by sharp temperature gradients (e.g. Pickart et al. 2010).

Dynamics of flow through Herald Canyon have received little attention, perhaps due to the dearth in observations. Pickart et al. (2010) analyze a set of synoptic surveys progressing northward through the Canyon, which show the winter layer thickened and switched from the western to the eastern flank of the canyon, consistent with theories of hydraulic control in straits. The observations suggest that hydraulic

control may be important in setting both the northward transport of winter water and the mixing, which can be significant, between summer and winter. Due to limited observations, whether and how Herald Canyon impacts shelf-break exchange is not well-known. Numerical modeling efforts (e.g., Chapman and Gawarkiewicz 1995; Gawarkiewicz and Chapman 1995; Chapman 2000) suggest that dense water created on the shelf and routed through canyons may be carried across the shelf break as deep gravity currents and episodic eddies, although such flows have yet to be observed in Herald Canyon. Similarly, the role of wind-driven circulation in this region is not fully understood.

6.4.2 Barrow Canyon

Barrow Canyon is located at the northeast corner of the Chukchi Sea at the juncture between the Chukchi Shelf and the Alaskan Beaufort Shelf where the shelf narrows dramatically. Due to a nearly right degree turn in the Alaskan coastline, the axis of the canyon is located parallel to the Alaskan coast on the Chukchi shelf, but perpendicular to the Beaufort shelf. The canyon stretches roughly 200 km from the shallow Chukchi (40 m deep) out across the Beaufort slope. Its cross-canyon scale is ~50 km; and, depths exceed 250 m. The complexities of the topography and coastline combined with wind forcing create a dynamic physical environment, which despite numerous observations is not fully understood.

Pacific Water, flowing northward along the coastline of Alaska, exits the Chukchi through Barrow Canyon. Similar to Herald Canyon, Barrow Canyon primarily transports Bering Winter Water in winter; however, its source is from the eastern Bering, which is relatively nutrient poor compared to western Bering water. In summer, water mass properties in Barrow Canyon vary, with contributions from warm, buoyant Alaskan Coastal Water, cold Bering Winter Water, fresh and cold melt water, and relatively warm, salty Arctic halocline water upwelled from the Beaufort (Mountain et al. 1976; Munchow and Carmack 1997; Weingartner et al. 1998). In addition, water from Herald Canyon can be re-routed through the head of Barrow Canyon after traveling eastward along the Chukchi shelf-break and around Hanna Shoal situated to the west of Barrow Canyon (e.g. Spall 2007).

Circulation in Barrow Canyon depends upon the large-scale pressure gradient, wind forcing, coastally-trapped waves, hydraulic control (of winter water), and (in summer) buoyancy forcing. Short-term variability (days-weeks) has been linked to wind forcing (Weingartner et al. 1998; Woodgate et al. 2005a) and shelf wave activity (Aagaard and Roach 1990). As Barrow Canyon is at a sharp change in shelf width, the scattering of shelf waves into shorter modes will likely also affect the complex and variable flow at the mouth of the canyon (Wilkin and Chapman 1987). In contrast, long-term variability (months) appears to be related to the large-scale pressure gradient between the Pacific and Arctic (Mountain et al. 1976). As with Herald Canyon, hydraulics and mixing may be a factor in the flow of dense winter water down Barrow Canyon (Pickart et al. 2005).

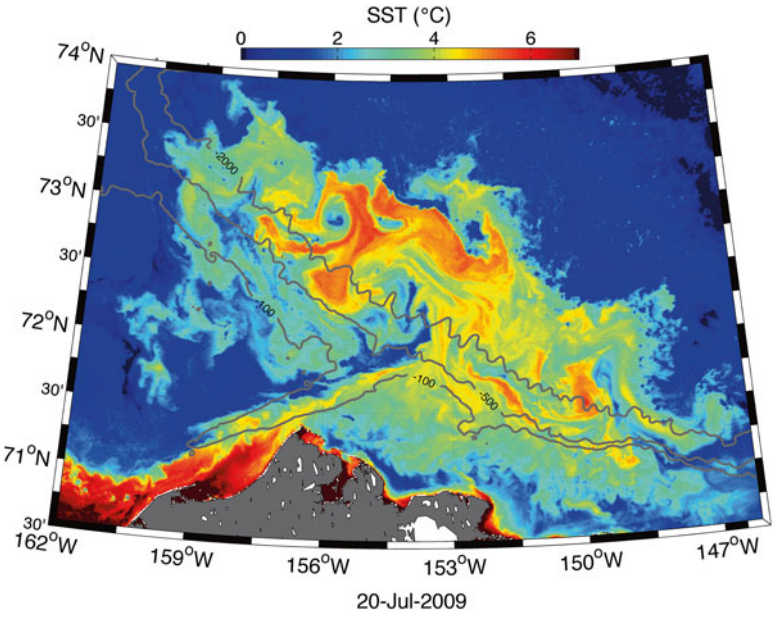

Fig. 6.9 Sea surface temperature (Modis Aqua) from 20 July 2009 in the vicinity of Barrow Canyon. The 100-, 500-, and 2,000-m isobaths are shown in *grey*

The momentum balance within Barrow Canyon is complicated. A secondary circulation in the across-shelf momentum equation results in a wedge shaped pycnocline (with a sharper, deeper interface on the shoreward side of the canyon) formed between the relatively warm, fresh surface water and cold salty winter water at depth (Signorini et al. 1997). This signature has also been seen in other observations (Pickart et al. 2005). Using a numerical model, Signorini et al. (1997) quantify terms in the along-shelf momentum balance, which is influenced strongly by the propagation of coastally-trapped waves initiated through temporal variability in the boundary conditions. The resultant interaction of a variable barotropic flow with canyon topography yields an up-canyon flow of deep water. Thus, both wind-driven local upwelling (e.g. Weingartner et al. 1998) and internal canyon dynamics (potentially affected by upstream changes in wind forcing) may result in up-canyon flow of Arctic halocline water.

The fate of the coastal current upon exiting the canyon depends upon wind conditions (Okkonen et al. 2009) and current stability. Sea surface temperature imagery shows instabilities that appear to emanate from the mouth of the canyon (Fig. 6.9). These dynamical processes are likely of importance to the shelf-basin flux of heat, fresh water, carbon, and nutrients, thus impacting the ecosystem, hydrography, and ice cover in the deep Arctic. A combination of mechanisms have been suggested as candidates for eddy formation in the vicinity of Barrow Canyon, including lateral boundary separation at Point Barrow (D'Asaro 1988), barotropic instability (Watanabe 2011), and outflow of relatively low potential vorticity water from the

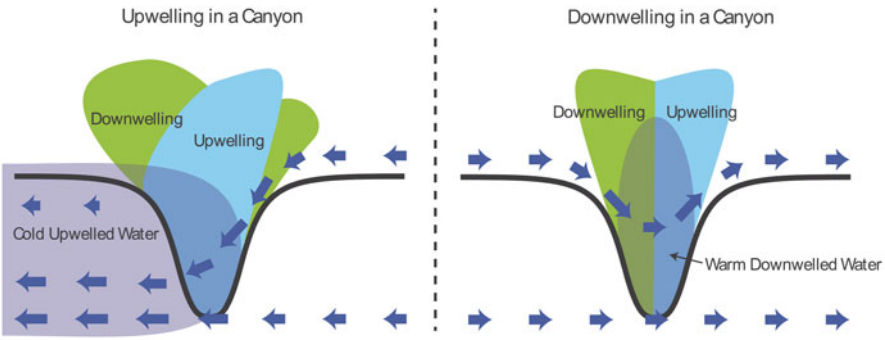

Fig. 6.10 Schematics showing canyon circulation during upwelling and downwelling winds after modeling results by Klinck (1996). Shown are approximate regions of upwelling (*blue*), downwelling (*green*), and cool upwelled water (*transparent purple*). *Blue arrows* are representative of horizontal currents

canyon (Shimada et al. 2001; Watanabe 2011). In addition, modeling efforts have shown that dense water formed in coastal polynyas is advected down Barrow Canyon and carried across the slope in eddies that form near the mouth of Barrow Canyon (Nguyen et al. 2012), in agreement with the idealized models of (e.g., Chapman 2000; Gawarkiewicz and Chapman 1995). The range of processes believed relevant in exchange near Barrow Canyon is indicative of several factors including strong seasonality in hydrographic and current properties, as well as complex topography and forcing (i.e., the large-scale flow of Pacific water, shelf wave activity, and local wind forcing).

6.4.3 Mackenzie Trough

Mackenzie Trough is located offshore of the Mackenzie River delta in between the Alaskan Beaufort Shelf and Mackenzie Shelf. This undersea canyon is roughly 200 km long, ~60-km wide, and ~400-m deep at its mouth. Circulation within the canyon is strongly influenced by wind forcing, and observations (Williams et al. 2006) suggest that the dynamics are in agreement with that expected for other canyons of the same dynamic scale as Mackenzie Trough for which the width is 2–3 times the internal Rossby radius (see Hyun 2004).

Upwelling of deep water in the canyon is correlated with northeasterly winds and is amplified in the canyon compared to the surrounding shelf (Carmack and Kulikov 1998). Upwelling winds result in an along-canyon pressure gradient at the canyon rim with a region of relatively high pressure near the mouth compared to that at the canyon head; across-isobath, onshore flow results from the along-canyon pressure gradient (for details see Klinck 1996). A schematic for upwelling wind-induced circulation following Klinck (1996) is shown in Fig. 6.10a, although not apparent in this schematic the strongest upwelling occurs near the head of the canyon. Also

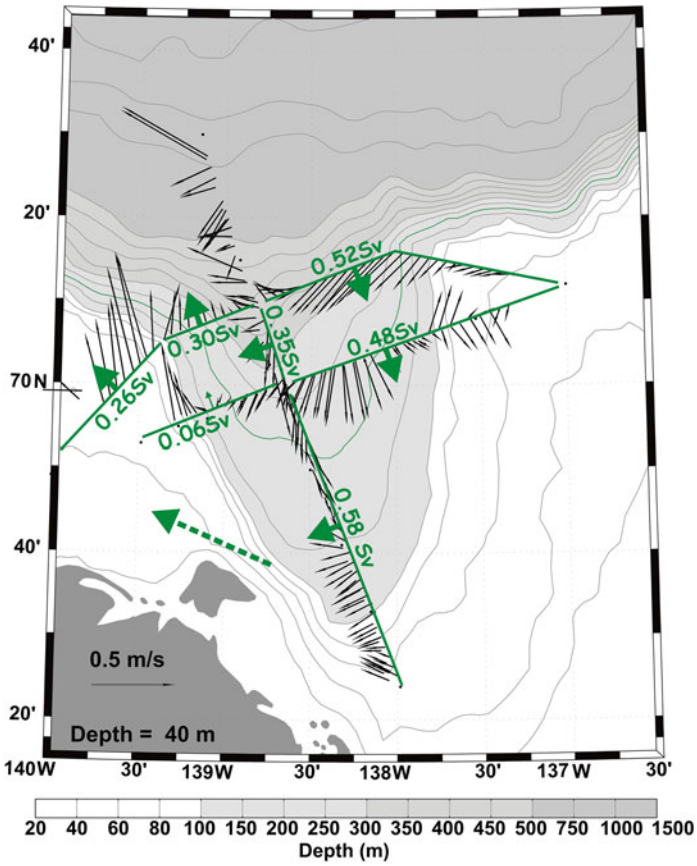

Fig. 6.11 Current data from Mackenzie Trough acquired during a strong upwelling wind event in September 2002 (see Williams et al. 2006 for further description). Data from 40 m deep are shown. Although flow fields are complex, the general tendency is up-canyon along the down-shelf (eastward) side and a return back along the canyon on the up-shelf (westward) side. Transports across each section (*green arrows*) show that there is much more inflow than outflow suggesting shelfbreak upwelling immediately north of Herschel Island (*dotted green arrow*) (Reproduced from Fig. 5 of Williams and Carmack 2012)

shown are velocity data from Mackenzie Trough (Fig. 6.11, reproduced from Fig. 9 in Williams et al. 2006). There is strong onshore flow on the down-shelf side of the canyon (reminiscent of the idealized modeling by Klinck 1996) but much weaker return flow on the up-shelf side of the canyon. Integration of the data to calculate transports shows that the flow crosses the head of the canyon and suggests it upwells onto the Alaskan Beaufort Shelf immediately north of Herschel Island. Data shown in Mathis et al. (2012) provide an example of this occurring.

An asymmetry exists in the comparison of upwelling and downwelling wind events, such that cross-shelf exchange within a canyon is much weaker in the case of downwelling (Klinck 1996). Downwelling winds result in regions of upwelling

and downwelling that tend to be symmetric about the canyon's axis and of small amplitude (Fig. 6.10b); in such cases, flow is primarily steered along-isobaths rather than across-isobaths (Klinck 1996). This asymmetry combined with the observation that under the influence of ice cover upwelling-favorable surface stresses are preferred (since downwelling favorable wind-forced ice motion in this region tends to be blocked by internal ice stress) results in a net flux of deep, nutrient-rich water on to the shelf (Williams et al. 2006). Observations from Kugmallit Valley, one of the many shallow valleys near Mackenzie Trough, suggest that enhanced cross-shelf transport may also be associated with less-pronounced topographic features that need not extend all the way to the shelf edge (Williams et al. 2008). These results suggest the possibility of many localized regions of enhanced exchange contributing to the overall physical setting and marine ecosystem on the Chukchi and Beaufort shelves.

6.5 Polynya-Formed Dense Shelf Water

Wind-driven polynyas occur when offshore wind pushes ice away from the coast or from the land-fast ice edge forming areas of recurrent open water in winter. The large heat flux to the atmosphere from the water leads to large amounts of ice formation and, as the brine is rejected from the forming sea ice, results in the creation of cold, salty dense shelf water in the polynya (for a review of polynya types and their forcing see Williams et al. 2007). The dense shelf water has a tendency to flow downhill and ultimately cross the shelf-break (Melling and Lewis 1982; Melling and Moore 1995). However, many factors – rotational control, bottom boundary layer processes, along-shelf flows, instabilities leading to eddies, and mixing with other water masses – all affect how and where this water crosses the shelf-break and dilute its properties (e.g. Gawarkiewicz 2000). We include a description of polynyas in Chukchi Sea as these are relatively well studied in terms of their effect on the ocean and they modify the waters that flow into Barrow Canyon.

One of the largest Arctic polynyas occurs in the Chukchi Sea along the Alaskan coast between Cape Lisburne and Point Barrow, forced by offshore winds during winter (e.g. Cavalieri and Martin 1994; Martin et al. 2004). This polynya lies along the pathway of Pacific Water inflow from the Bering Strait that goes via Barrow Canyon into the Canada Basin. In general, heat loss over a coastal polynya is one or two orders of magnitude larger than that over thick ice (Maykut 1978), thus coastal polynyas are very active areas of ice formation. Brine rejection from this rapid ice formation in the polynya increases the salinity of Pacific Winter Water flowing through Barrow Canyon. The maximum salinity observed is up to 34.5 psu and is potentially the densest water that forms in the western Arctic Ocean (e.g. Weingartner et al. 1998, 2005) thus we call it *hyper-saline* Pacific Winter Water. Transport of winter water through Barrow Canyon into the basin is estimated to be 0.1–0.3 Sv from mooring and shipboard data (Woodgate et al. 2005a; Pickart et al. 2005; Itoh et al. 2012).

The formation of hyper-saline Pacific Winter Water is dependent on the occurrence of the Barrow – Cape Lisburne polynya. Thus, accurate observation of the polynya's area is essential, as the salt flux to the Pacific Winter Water is due to ice formation in the polynya. Martin et al. (2004) and Tamura and Ohshima (2011) examined an algorithm that estimates the thin ice thickness within a polynya using Special Sensor Microwave/Imager (SSM/I) data, and, using that, estimated sea ice production and salt flux within the coastal polynyas via a heat budget. Tamura and Ohshima (2011) estimated annual accumulated sea ice production is 6–14 m/year within the Barrow – Cape Lisburne polynya for 1992–2007, far larger than typical annual sea ice production in the Chukchi Sea of ~2 m/year. Sea-ice production in the Barrow-Cape Lisburne polynya can vary from year to year by as much as a factor of 3–4 (Martin et al. 2004; Tamura and Ohshima 2011)

Winsor and Chapman (2002) examined dense water formation for the coastal polynyas on the Chukchi shelf using an ocean model for the winters of the 1978–1998 period. They showed that the accumulated ice growth is 9–15 m/year over the polynya area and the maximum salinity anomaly is typically 1–1.5 psu. They proposed that its interannual variability is high and that most of the observed variability can be explained by the varying wind field. Winsor and Chapman (2002) also suggested that variation in the initial salinity of the Chukchi shelf, which is determined by Bering Strait through-flow, is equally important to the salinization within the polynya and thus in determining the interannual variability of dense water formation. Martin et al. (2004) compared the ice volume, derived using the SSM/I algorithm, with that obtained by Winsor and Chapman (2002) based on Pease's (1987) analytical model, and showed a significant difference, even in relative variabilities of sea ice production between the two estimates. Martin et al.'s (2004) results suggested that interannual variability of Barrow – Cape Lisburne polynya cannot be explained by simple analytical polynya model developed by Pease (1987), implying that Pease's assumption of free-drift of ice does not apply adequately in this polynya.

Kawaguchi et al. (2011) examined winter water formation for the winters of 1992–2006 using an ocean model forced by wind and surface salinity flux derived from SSM/I thin-ice thickness estimate. Their experiment shows that the Barrow Cape Lisburne polynya preferentially opens under strong northeasterly wind conditions. Additionally, under the northeasterly wind conditions, northward through-flow across Barrow Canyon tends to be reduced and results in salinity build up and ultimately in greater enhancement of salinity in water carried into the Canada Basin. Such wind conditions are established when the Beaufort high pressure system is intensified and Aleutian low pressure system is located west of its mean position. Kawaguchi et al. (2011) also pointed out that the ice production in the Kotzebue Sound coastal polynya is comparable to that in the Barrow – Cape Lisburne polynya, and it is also crucially important for salinity enhancement of winter water transported through Barrow Canyon. Together with moored salinity in the Bering Strait from Woodgate et al. (2005b), Kawaguchi et al.'s (2011) model results show that the salinity across the Barrow and Herald Canyons is 32.9 ± 0.8 psu and 32.7 ± 0.3 psu, respectively. Through-flow via Herald Valley is estimated to have smaller and more intermittent salinity enhancement than that via Barrow Canyon. This is expected

since winter water carried via Herald Valley is less likely to have been modified by coastal polynyas.

Hyper-saline Pacific Winter Water formation within the Barrow – Cape Lisburne polynya and its interannual variability have been mostly examined by heat budget analysis and modeling, with limited oceanographic observational studies. From oceanographic observations during spring in 1975, Garrison and Becker (1976) found that highly saline water (up to 34 psu) is capable of ventilating the lower halocline layer (see Fig. 6.5 for a profile through the halocline), and suggested that it flows into the Beaufort Sea via Barrow Canyon. Weingartner et al. (1998, 2005) investigated circulation and water modification processes in the Chukchi Sea using mooring and shipboard data between 1992 and 1995. Weingartner et al. (2005) found that winter water salinity values on the Hanna Shoal ranged widely: from 31.3 to 34.5 psu in the winter of 1993–1994, and from 31.5 to 32.7 in the winter of 1992–1993. They suggested that reduced fall and winter ice cover and a large winter polynya area in 1993–1994 result in enhancement of hyper-saline winter water production. Weingartner et al. (2005) also pointed out that hyper-saline winter water derived from the Barrow – Cape Lisburne polynya exits the Chukchi Shelf into the basin not only via the Barrow Canyon but also via the Central Channel.

Itoh et al. (2012) examined the interannual variability of Pacific Winter Water both upstream in the northeastern Chukchi Sea, using moored observations, and downstream in the Canada Basin, using hydrographic data for 2000–2006. They proposed that the formation of hyper-saline Pacific Winter Water depends jointly on the salinity of incoming water at the Bering Strait gateway and the on occurrence of the Barrow – Cape Lisburne polynya. A large transport of cold and saline winter water via Barrow Canyon was observed in the winters of 2000/2001 and 2001/2002. In the former winter, enhanced ice formation in the polynya contributed to the increased salinity of Pacific Winter Water entering the basin, whereas in the latter winter, the high salinity of water entering the Bering Strait gateway was essential in delivering saline Pacific Winter Water to the basin. Itoh et al. (2012) also found that warm water within the polynya constrained ice formation in the winter of 2003/2004, resulting in reduced transport of hyper-saline winter water despite the fact that the coastal polynya was frequently open. Figure 6.12 shows that subsurface water at $S = 31.5$ psu, corresponding to the core of Pacific Summer Water, was above freezing point even in mid winter, possibly due to up-canyon flow from the basin onto to the Chukchi Shelf.

The Barrow Cape Lisburne polynya is believed to be a wind-driven polynya, and such polynyas are very active regions of ice formation when maintained by offshore wind. However, accumulated upper ocean heat in the Arctic Ocean due to global warming could change this situation. Woodgate et al. (2006) showed that heat flux through the Bering Strait increased from 2002 to 2004 due to the warming of Pacific Summer Water. Steele et al. (2008) also reported increased heat in the upper layer of the Chukchi Sea after 2000. In addition, less extensive sea ice has been observed in the Arctic Ocean during summers in recent years (Serreze et al. 2007) and the absence of ice cover for a longer season in the Chukchi Sea will promote surface warming. Figure 6.13 shows that surface temperature through Barrow Canyon has

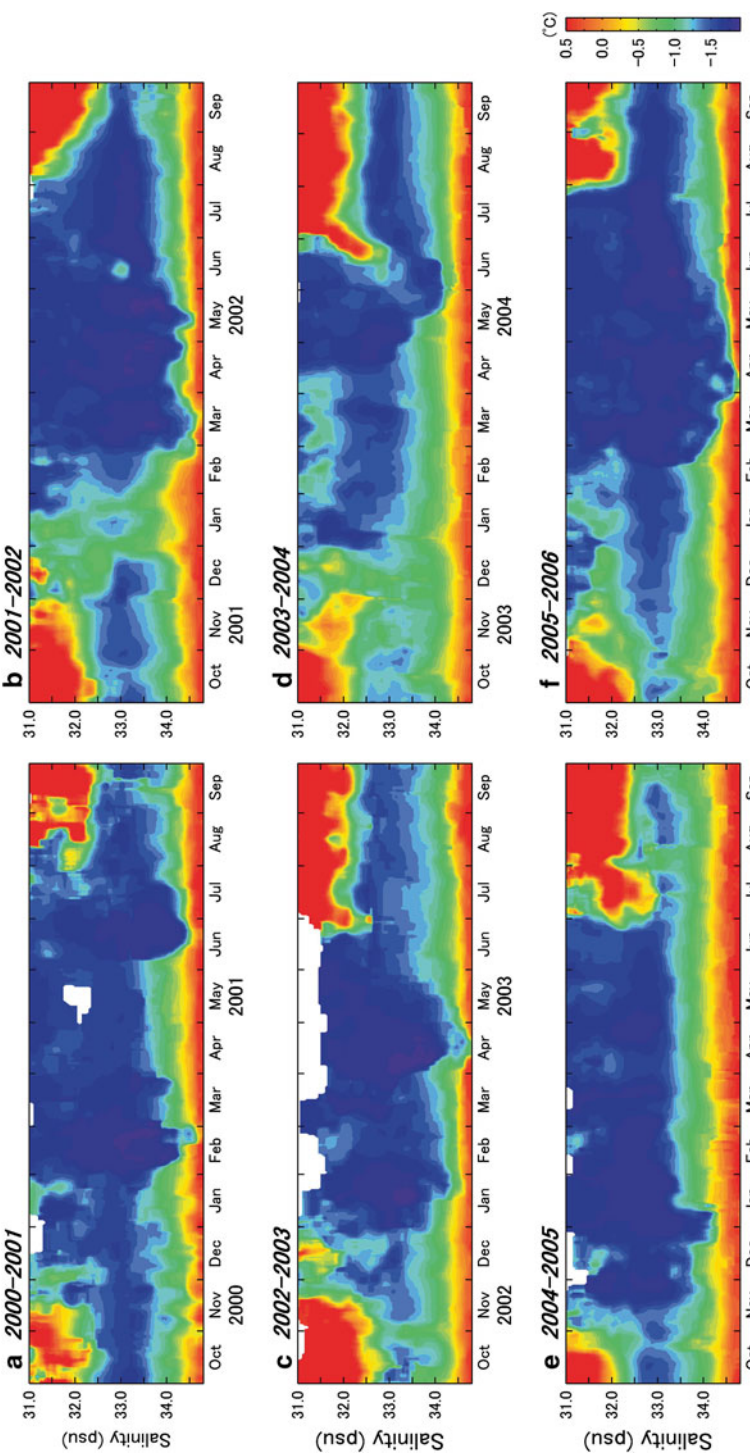

Fig. 6.12 Time series of temperature plotted as a function of salinity at the mouth of Barrow Canyon obtained by combining data from moorings BCE, BCC, BCW that spanned the mouth of the canyon (see Fig. 6.1c for locations) and contained instruments from ~30 m deep to close to the sea-floor. Panel (**a**) 2000–2001, (**b**) 2001–2002, (**c**) 2002–2003, (**d**) 2003–2004, (**e**) 2004–2005, and (**f**) 2005–2006 (Adapted from Fig. 13 of Itoh et al. (2012) with permission from Springer)

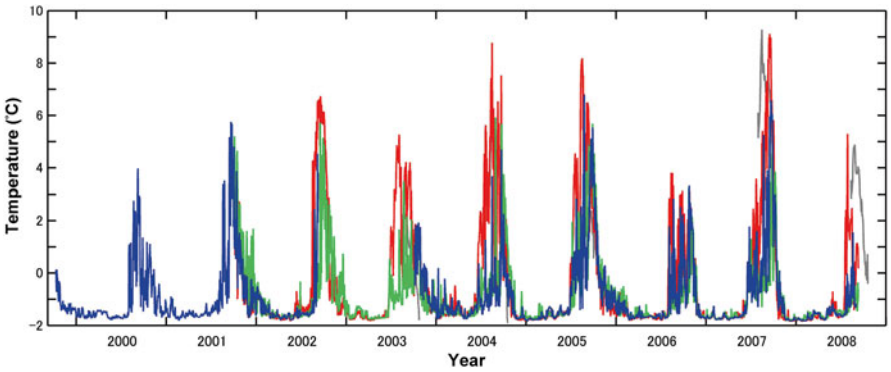

Fig. 6.13 Time series of upper ocean temperature (40 m) from the mouth of Barrow Canyon obtained from moorings BCE, BCC and BCW (see Fig. 6.1c for locations). *Red, blue and green curves* indicate data from the eastern (BCE), central (BCC) and western (BCW) canyon. *Gray curves* indicate SST data derived from microwave satellite AMSRE

increased since early 2000s. These results, showing warming, suggest an increase in the time in autumn that heat loss merely cools the water column, rather than leading to the formation of sea ice. Further, the water column within the polynya was warm enough to constrain ice formation even in mid-winter of 2003/2004, as suggested by Itoh et al. (2012). Although this warm water constrained ice formation in mid-winter in this polynya, it must be a local, advective phenomenon as ice formation does occur in the Bering and Chukchi Seas in winter following rapid heat loss in autumn. In addition, Wang et al. (2012) predict that there will always be ice formation on the Bering Shelf in winter under IPCC climate warming scenarios.

6.6 Summary

6.6.1 Bering Shelf-Break

Much of our detailed understanding of the Bering shelf-break comes from numerical models. These results need support from complementary observational data, in particular to assess the relative importance of wind-driven exchange, large slope eddies, canyon dynamics, and internal tides that propagate across the basin from the Aleutians. Such observational data could be achieved by deployment of high- and medium-resolution mooring arrays across the shelf-break and upper slope. Recent high-resolution observations by BEST-BSIERP increased our understanding of processes on the shelf and we suggest similar effort needs to be focused on the shelf-break, at a range of temporal and spatial scales. The evident success of the high-resolution array deployed across the Alaskan Beaufort shelf-break (Pickart 2004) could be emulated here.

6.6.2 Chukchi/Beaufort Shelf-Break

Transport via current instabilities and wind-driven exchange are important components of shelf-break exchange at the Chukchi/Beaufort shelf-break. However, many questions remain regarding how Pacific Water is carried into the deep basin. The role of time-varying winds and instabilities in the presence of a complex coastline (e.g. Point Barrow) and topography (canyons) needs further study. Long-term, high-frequency observations detailing circulation in canyons, which are thought to be important avenues for enhanced exchange, would further add to our understanding. In addition, since the data suggest that much of the off shelf flow of Pacific Water, crosses the Chukchi shelf-break, further research on the mechanisms of shelf-break exchange there would greatly enhance our understanding of how Pacific-origin water moves into the Canadian Basin. The Chukchi shelf-break is much more rounded than the Alaskan Beaufort shelf-break and possibly behaves substantially differently because of this. Considering the impact that cross-shelf exchange has on the deep basin hydrography and ice cover, addressing these unknowns is key to understanding the current state of the Arctic ecosystem and how this system might evolve under climate change.

Observational work in the Bering, Chukchi and Beaufort Seas has additional logistical complexity as these seas border Russia, Canada and the USA. Our growing comprehensive understanding of the Pacific-Arctic Region can only be nurtured though continued international collaboration that is able to transcend cultural and bureaucratic limitations.

Acknowledgements Support for W. Williams was provided by Fisheries and Oceans Canada. E. Shroyer was supported as a WHOI Postdoctoral Scholar through the WHOI Ocean and Climate Change Institute. Funding support for contributions by J. Clement Kinney and W. Maslowski was provided by multiple grants from the Climate Change Prediction Program of the Department of Energy, the Arctic System Science (ARCSS) Program of the National Science Foundation (NSF), and the Office of Naval Research. Funding for M. Itoh was provided by Japan Agency for Marine-Earth Science and Technology. We thank Robert Pickart and Albert Plueddemann and Seth Danielson for insightful discussions regarding circulation in the Chukchi-Beaufort region. We also thank the editors of this book and two anonymous reviewers for insightful comments, which improved an earlier version of this manuscript.

References

Aagaard K, Roach AT (1990) Arctic ocean-shelf exchange: measurements in Barrow Canyon. J Geophys Res 95:18163–18175

Aagaard K, Coachman LK, Carmack EC (1981) On the halocline of the Arctic Ocean. Deep-Sea Res 28:529–545

Aagaard K, Weingartner TJ, Danielson SL, Woodgate RA, Johnson GC, Whitledge T (2006) Some controls on flow and salinity in Bering Strait. Geophys Res Lett 33:L19602. doi:10.1029/2006GL026612

Carmack EC, Kulikov EA (1998) Wind-forced upwelling and internal Kelvin wave generation in Mackenzie Canyon, Beaufort Sea. J Geophys Res 103:18447–18458

Cavalieri D, Martin S (1994) The contribution of Alaskan, Siberian, and Canadian coastal polynyas to the cold halocline layer of the Arctic Ocean. J Geophys Res 99:18343–18362
Chapman DC (2000) The influence of an alongshelf current on the formation and offshore transport of dense water from a coastal polynya. J Geophys Res 105(C10):24007–24019. doi:10.1029/2000JC000296
Chapman DC, Gawarkiewicz G (1995) Offshore transport of dense shelf water in the presence of a submarine canyon. J Geophys Res 100(C7):13373–13387. doi:10.1029/95JC00890
Clement Kinney J, Maslowski W, Okkonen S (2009) On the processes controlling shelf–basin exchange and outer shelf dynamics in the Bering Sea. Deep Sea Res Part II Top Stud Oceanogr 56(17):1351–1362. doi:10.1016/j.dsr2.2008.10.023
Coachman LK, Aagaard K, Tripp RB (1975) Bering Strait: the regional physical oceanography. University of Washington Press, Seattle, p 172
Cooper LW, Whitledge TE, Grebmeier JM, Weingartner TJ (1997) The nutrient, salinity, and stable oxygen isotope composition of Bering and Chukchi Seas waters in and near the Bering Strait. J Geophys Res 102:12563–12573
D'Asaro EA (1988) Generation of submesoscale vortices: a new mechanism. J Geophys Res 93:6685–6693
Danielson S, Hedstrom K, Aagaard K, Weingartner T, Churchitser E (2012) Wind-induced reorganization of the Bering shelf circulation. Geophys Res Lett 39:L08601. doi:10.1029/2012GL051231
Garrison GR, Becker P (1976) The Barrow Submarine Canyon: a drain for the Chukchi Sea. J Geophys Res 81:4445–4453. doi:10.1029/JC081i024p04445
Gawarkiewicz G (2000) Effects of ambient stratification and shelf break topography on offshore transport of dense water on continental shelves. J Geophys Res 105(C2):3307–3324
Gawarkiewicz G, Chapman DC (1995) A numerical study of dense water formation and transport on a shallow, sloping continental shelf. J Geophys Res 100(C3):4489–4507. doi:10.1029/94JC01742
Hughes FW, Coachman LK, Aagaard K (1974) Circulation, transport, and water exchange in the western Bering Sea. In: Hood DW, Kelley EJ (eds) Oceanography of the Bering Sea, with emphasis on renewable resources, Publ. 2. Institute of Marine Science, University of Alaska Fairbanks, Fairbanks
Huthnance JM (1995) Circulation, exchange and water masses at the ocean margin: the role of physical processes at the shelf edge. Prog Oceanogr 35:353–431
Hyun KH (2004) The effect of submarine canyon width and stratification on coastal circulation and across shelf exchange. PhD thesis, Old Dominion University
Itoh M, Shimada K, Kamoshida T, McLaughlin F, Carmack E, Nishino S (2012) Interannual variability of Pacific Winter Water inflow through Barrow Canyon from 2000 to 2006. J Oceanogr 68:575–592. doi:10.1007/s10872-012-0120-1
Karl HA, Carlson PR (1987) Surface current patterns suggested by suspended sediment distribution over the outer continental margin Bering Sea. Mar Geol 74:301–308
Kawaguchi Y, Tamura T, Nishino S, Kikuchi T, Itoh M, Mitsudera F (2011) Numerical study of winter water formation estimation in the Chukchi Sea: roles and impacts of coastal polynya. J Geophys Res. doi:10.1029/2010JC006606
Kinder TH, Coachman LK (1978) The front overlying the slope in the eastern Bering Sea. J Geophys Res 83:4551–4559
Kinder TH, Coachman LK, Galt JA (1975) The Bering slope current system. J Phys Oceanogr 5:231–244
Kinder TH, Schumacher JD, Hansen DV (1980) Observation of a baroclinic eddy: an example of mesoscale variability in the Bering Sea. J Phys Oceanogr 101:1228–1245
Kinder TH, Chapman DC, Whitehead JA (1986) Westward intensification of the mean circulation on the Bering Sea Shelf. J Phys Oceanogr 16:1217–1229. doi:10.1175/15200485
Kirillova EP, Stepanov OV, Weingartner TJ (2001) Distribution and variability of nutrients in the northwestern part of the Chukchi Sea. In: Proceedings of the Arctic Regional Centre 3

Klinck JM (1996) Circulation near submarine canyons: a modeling study. J Geophys Res 101:1211–1223
Krishfield RA, Plueddemann AJ, Honjo S (2002) Eddies in the Arctic Ocean from IOEB ADCP data. Woods Hole Oceanographic Institution technical report WHOI-2002-09
Krishfield R, Toole J, Proshutinsky A, Timmermans M-L (2008) Automated ice-tethered profilers for seawater observations under pack ice in all seasons. J Atmos Oceanic Tech 25:2091–2095
Manley TO, Hunkins K (1985) Mesoscale eddies of the Arctic Ocean. J Geophys Res 90(C3):4911–4930
Martin S, Drucker R (1997) The effect of possible Taylor columns on the summer ice retreat in the Chukchi Sea. J Geophys Res 102:10473–10482
Martin S, Drucker R, Kwok R, Holt B (2004) Estimation of the thin ice thickness and heat flux for the Chukchi Sea Alaskan coast polynya from Special Sensor Microwave/Imager data, 1990–2001. J Geophys Res 109:C10012. doi:10.1029/2004JC002428
Maslowski W, Marble D, Walczowski W, Schauer U, Clement JL, Semtner AJ (2004) On climatological mass, heat, and salt transports through the Barents Sea and Fram Strait from a pan-Arctic coupled ice-ocean model simulation. J Geophys Res 109:C03032. doi:10.1029/2001JC001039
Maslowski W, Clement Kinney J, Okkonen SR, Osinski R, Roberts AF, Williams W (2014) Chapter 5: The large scale ocean circulation and physical processes controlling Pacific-Arctic interactions. In: Grebmeier JM, Maslowski W (eds) The Pacific Arctic region: ecosystem status and trends in a rapidly changing environment. Springer, Dordrecht, pp 101–132
Mathis JT, Pickart RS, Hansell DA, Kadko D, Bates NR (2007) Eddy transport of organic carbon and nutrients from the Chukchi Shelf: impact on the upper halocline of the western Arctic Ocean. J Geophys Res 112, C05011. doi:10.1029/2006JC003899
Mathis JT, Pickart RS, Byrne RH, McNeil CL, Moore GWK, Juranek LW, Liu X, Ma J, Easley RA, Elliot MM, Cross JN, Reisdorph SC, Bahr F, Morison J, Lichendorf T, Feely RA (2012) Storm-induced upwelling of high pCO_2 waters onto the continental shelf of the western Arctic Ocean and implications for carbonate mineral saturation states. Geophys Res Lett 39:L07606. doi:10.1029/2012GL051574
Maykut G (1978) Energy exchange over young sea ice in the central Arctic. J Geophys Res 83:3646–3658
Melling H, Lewis EL (1982) Shelf drainage flows in the Beaufort Sea and their effect on the Arctic Ocean pycnocline. Deep Sea Res Part A 29:967–985
Melling H, Moore RM (1995) Modification of halocline source waters during freezing on the Beaufort Sea shelf: evidence from oxygen isotopes and dissolved nutrients. Cont Shelf Res 15:89–113
Mizobata K, Saitoh SI (2004) Variability of Bering Sea eddies and primary productivity along the shelf edge during 1998–2000 using satellite multi-sensor remote sensing. J Mar Syst 50:101–111
Mizobata K, Wang J, Saitoh SI (2006) Eddy-induced cross-slope exchange maintaining summer high productivity of the Bering Sea shelf break. J Geophys Res 111:C10017
Mountain DG, Coachman LK, Aagaard K (1976) On the flow through Barrow Canyon. J Phys Oceanogr 6:461–470
Muench R, Gunn J, Whitledge T, Schlosser P, Smethie W Jr (2000) An Arctic Ocean cold core eddy. J Geophys Res 105:23997–24006. doi:10.1029/2000JC000212
Munchow A, Carmack EC (1997) Synoptic flow and density observations near an Arctic shelf break. J Phys Oceanogr 27:1402–1419
Nguyen AT, Kwok R, Menemenlis D (2012) Source and pathway of the western Arctic upper halocline in a data-constrained coupled ocean and sea ice model. J Phys Oceanogr 42:802–823
Nikolopoulos A, Pickart RS, Fratantoni PS, Shimada K, Torres DJ, Jones EP (2009) The western Arctic boundary current at 152°W: structure, variability, and transport. Deep-Sea Res Part II 56:1164–1181. doi:10.1016/j.dsr2.2008.10.014

Okkonen SR (2001) Altimeter observations of the Bering Slope Current eddy field. J Geophys Res 106:2465–2476
Okkonen SR, Schmidt GM, Cokelet ED, Stabeno PJ (2004) Satellite and hydrographic observations of the Bering Sea 'Green Belt'. Deep-Sea Res Part II 51:1033–1051
Okkonen SR, Ashjian CJ, Campbell RG, Maslowski W, Clement Kinney JL, Potter R (2009) Intrusion of warm Bering/Chukchi waters onto the shelf in the western Beaufort Sea. J Geophys Res. doi:10.1029/2008JC004870
Paluszkiewicz T, Niebauer HJ (1984) Satellite observations of circulation in the eastern Bering Sea. J Geophys Res 89:3663–3678
Pease CH (1980) Eastern Bering Sea ice processes. Mon Weather Rev 108:2015–2023
Pease CH (1987) The size of wind-driven coastal polynyas. J Geophys Res 92:7049–7059. doi:10.1029/JC092iC07p07049
Pickart RS (2004) Shelf-break circulation in the Alaskan Beaufort Sea: mean structure and variability. J Geophys Res 109:C04024. doi:10.1029/2003JC001912
Pickart RS, Stossmeister G (2008) Outflow of Pacific water from the Chukchi Sea to the Arctic Ocean. Chin J Polar Sci 19:135–148
Pickart RS, Weingartner TJ, Pratt LJ, Zimmermann S, Torres DJ (2005) Flow of winter-transformed Pacific water into the Western Arctic. Deep-Sea Res Part II 52:3175–3198
Pickart RS, Moore GWK, Torres DJ, Fratantoni PS, Goldsmith RA, Yang J (2009) Upwelling on the continental slope of the Alaskan Beaufort Sea: storms, ice, and oceanographic response. J Geophys Res 114:C00A13. doi:10.1029/2008JC005009
Pickart RS, Pratt LJ, Torres DJ, Whitledge TE, Proshutinsky AY, Aagaard K, Agnew TA, Moore GWK, Dail HJ (2010) Evolution and dynamics of the flow through Herald Canyon in the western Chukchi Sea. Deep-Sea Res Part II 57:5–26. doi:10.1016/j.dsr2.2009.08.002
Pickart R, Spall M, Moore G, Weingartner T, Woodgate R, Aagaard K, Shimada K (2011) Upwelling in the Alaskan Beaufort Sea: atmospheric forcing and local versus non-local response. Prog Oceanogr 88:78–100. doi:10.1016/j.pocean.2010.11.005
Pickart RS, Spall MA, Mathis JT (2013a) Dynamics of upwelling in the Alaskan Beaufort Sea and associated shelf-basin fluxes. Deep Sea Res Part I: Oceanogr Res Pap 76:35–51. doi:10.1016/j.dsr.2013.01.007, ISSN 0967–0637
Pickart RS, Schulze LM, Moore GWK, Charette MA, Arrigo KR, van Dijken G, Danielson SL (2013b) Long-term trends of upwelling and impacts on primary productivity in the Alaskan Beaufort Sea. Deep-Sea Res 79:106–121
Proshutinsky A, Timmermans M-L, Ashik I, Beszczynska-Moeller A, Carmack E, Frolov I, Itoh M, Kikuchi T, Krishfield R, McLaughlin F, Rabe B, Schauer U, Shimada K, Sokolov V, Steele M, Toole J, Williams W, Woodgate R, Yamamoto-Kawai M, Zimmermann S (2011) The Arctic. In: Blunden J, Arndt DS, Baringer MO (eds) State of the climate in 2010. Bulletin of the American Meteorological Society 92(6), S143–S160
Schumacher JD, Reed RK (1992) Characteristics of currents over the continental slope of the eastern Bering Sea. J Geophys Res 97:9423–9433
Schumacher JD, Stabeno PJ (1994) Ubiquitous eddies of the eastern Bering Sea and their coincidence with concentrations of larval Pollock. Fish Ocean 3:182–190
Serreze M, Holland M, Stroeve J (2007) Perspective on the Arctic's shrinking sea ice cover. Science 315:1533–1536
Shimada K, Carmack EC, Hatakeyama K, Takizawa T (2001) Varieties of shallow temperature maximum waters in the western Canadian Basin of the Arctic Ocean. Geophys Res Lett 28:3441–3444
Shimada K, Kamoshida T, Itoh M, Nishino S, Carmack E, McLaughlin FA, Zimmermann S, Proshutinsky A (2006) Pacific Ocean inflow: influence on catastrophic reduction of sea ice cover in the Arctic Ocean. Geophys Res Lett 33:L08605. doi:10.1029/2005GL025624
Signorini SR, Munchow A, Haidvogel D (1997) Flow dynamics of a wide Arctic canyon. J Geophys Res 102:18661–18680

Spall MA (2007) Circulation and water mass transformation in a model of the Chukchi Sea. J Geophys Res 112:C05025. doi:10.1029/2005JC003364
Spall MA, Pickart RS, Fratantoni P, Plueddemann A (2008) Western Arctic Shelf-break eddies: formation and transport. J Phys Oceanogr 38:1644–1668. doi:10.1175/2007JPO3829.1
Stabeno PJ, van Meurs P (1999) Evidence of episodic onshelf flow in the southeast Bering Sea. J Geophys Res 104:29715–29720
Stabeno PJ, Schumacher JD, Salo SA, Hunt GL Jr, Flint M (1999) Physical environment around the Pribilof Islands. In: Loughlin TR, Ohtani K (eds) Dynamics of the Bering Sea, AK-SG-99-03. University of Alaska Sea Grant, Fairbanks
Steele M, Ermold W, Zhang J (2008) Arctic Ocean surface warming trends over the past 100 years. Geophys Res Lett. doi:10.1029/2007GL031561
Tamura T, Ohshima KI (2011) Mapping of sea ice production in the Arctic coastal polynyas. J Geophys Res. doi:10.1029/2010JC006586
Timmermans M, Toole J, Proshutinsky A, Krishfield R, Plueddemann A (2008) Eddies in the Canada Basin, Arctic Ocean, observed from ice-tethered profilers. J Phys Oceanogr 38:133–145
Toole JM, Timmermans ML, Perovich DK, Krishfield RA, Proshutinsky A, Richter-Menge JA (2010) Influences of the ocean surface mixed layer and thermohaline stratification on Arctic Sea ice in the central Canada Basin. J Geophys Res 115:C10018. doi:10.1029/2009JC005660
Toole JM, Krishfield RA, Timmermans M-L, Proshutinsky A (2011) The Ice-Tethered Profiler: Argo of the Arctic. Oceanography 24(3):126–135
von Appen W-J, Pickart RS (2011) Two configurations of the Western Arctic shelf-break current in summer. J Phys Oceanogr 42:329–351. doi:10.1175/JPO-D-11-026.1
Wang M, Overland JE, Stabeno P (2012) Future climate of the Bering and Chukchi Seas projected by global climate models. Deep-Sea Res Part II 65–70:46–57
Watanabe E (2011) Beaufort shelf break eddies and shelfbasin exchange of Pacific summer water in the western Arctic Ocean detected by satellite and modeling analyses. J Geophys Res 116:C08034. doi:10.1029/2010JC006259
Watanabe E, Hasumi H (2009) Pacific water transport in the Western Arctic Ocean simulated by an eddy-resolving coupled sea ice–ocean model. J Phys Ocean 39:2194–2211. doi:http://dx.doi.org/10.1175/2009JPO4010.1
Weingartner TJ, Cavalieri DJ, Aagaard K, Sasaki Y (1998) Circulation, dense water formation, and outflow on the northeast Chukchi shelf. J Geophys Res 103:7647–7662. doi:10.1029/98JC00374
Weingartner TJ, Aagaard K, Woodgate R, Danielson S, Sasaki Y, Cavalieri DJ (2005) Circulation on the north central Chukchi Sea shelf. Deep-Sea Res Part II 52:3150–3174
Wilkin JL, Chapman DC (1987) Scattering of continental shelf waves at a discontinuity in shelf width. J Phys Oceanogr 17:713–724
Williams WJ, Carmack EC (2012) Physical oceanography. In: Burn CR (ed) Herschel Island Qikiqtaruk – a natural and cultural history of Yukon's Arctic island. Wildlife Management Advisory Council (North Slope)
Williams WJ, Carmack EC, Shimada K, Melling H, Aagaard K, Macdonald RW, Ingram RG (2006) Joint effects of wind and ice motion in forcing upwelling in Mackenzie Trough, Beaufort Sea. Cont Shelf Res 26:2352–2366. doi:10.1016/j.csr.2006.06.012
Williams WJ, Carmack EC, Ingram RG (2007) Physical oceanography of polynyas. In: Smith WO Jr, Barber DG (eds) Polynyas: windows to the world, vol 74, Elsevier oceanography series. Elsevier, Amsterdam
Williams WJ, Melling H, Carmack EC, Ingram RG (2008) Kugmallit Valley as a conduit for cross-shelf exchange on the Mackenzie Shelf in the Beaufort Sea. J Geophys Res 113:C02007. doi:10.1029/2006JC003591
Winsor P, Chapman DC (2002) Distribution and interannual variability of dense water production from coastal polynyas on the Chukchi shelf. J Geophys Res. doi:10.1029/2004JC000984

Winsor P, Chapman DC (2004) Pathways of Pacific water across the Chukchi Sea: a numerical model study. J Geophys Res 109:C03002. doi:10.1029/2003JC001962

Woodgate RA, Aagaard K, Weingartner TJ (2005a) A year in the physical oceanography of the Chukchi Sea: moored measurements from autumn 1990–1991. Deep-Sea Res Part II 52:3116–3149

Woodgate R, Aagaard K, Weingartner T (2005b) Monthly temperature, salinity, and transport of the Bering Strait flow. Geophys Res Lett 32:L04601. doi:10.1029/2004GL021880

Woodgate R, Aagaard K, Weingartner T (2006) Interannual changes in the Bering Strait fluxes in volume, heat and freshwater between 1991 and 2004. Geophys Res Lett 33:L15609. doi:10.1029/2006GL026931

Woodgate RA, Weingartner T, Lindsay R (2010) The 2007 Bering Strait oceanic heat flux and anomalous Arctic sea-ice retreat. Geophys Res Lett 37:L01602. doi:http://dx.doi.org/10.1029/2009GL041621

Yang J (2006) The seasonal variability of the Arctic ocean Ekman transport and its role in the mixed layer heat and salt fluxes. J Climate 19:5366–5387